Journal of Engineering Science and Technology
Vol. 13, No. 2 (2018) 409 - 420

BIOSYNTHESIS AND CHARACTERIZATION OF ZnO NANOPARTICLES USING RICE BRAN EXTRACT AS LOW-COST TEMPLATING AGENT

IS FATIMAH

Chemistry Department, Faculty of Mathematics and Natural Sciences, Universitas Islam Indonesia. Kampus Terpadu UII Jl. Kaliurang Km 14, Sleman, Yogyakarta, Indonesia
E-mail: isfatimah@uii.ac.id

Abstract

ZnO nanoparticles (ZnO NPs) is one of important material in nanotechnology. Refer to green chemistry principles, the use of plant extract as reagent for nanoparticle synthesis has been highlighted. In present work, biosynthesis of ZnO nanoparticles (ZnO NPs) using rice bran as template, is discussed. The synthesis was conducted by refluxing ethanolic extract of rice bran powder with zinc acetate precursor followed by drying and calcination due to differential thermal analysis-thermal gravimetric (DTA-TGA) analysis. The synthesized ZnO NPs was characterized using x-ray diffraction (XRD), scanning electron microscopy (SEM), transmission electrone microscope (TEM), diffuse reflectance-Ultra Violet (DRS-UV) spectrophotometry and gas sorption analyzer. The data shows that ZnO nanoparticles were formed with the mean particle size of 17.16 nm and the band gap energy of 3.18 eV. The material demonstrates the photocatalytic activity in bromo phenol blue (BPB) photodegradation and antibacterial activity against *Escherichia coli*, *Staphylococcus aureus* and *Pseudomonas aeruginosa* bacteria.

Keywords: ZnO NPs, Biosynthesis, Rice bran, Photocatalyst.

1. Introduction

ZnO has been extensively studied as a photocatalyst and semiconductor material instead of TiO_2 for some environmental remediation applications. Its low cost, excellent electrochemical stability, and high electron mobility properties are some advantages that push some investigations up to enhance the performance. In other side the chemical instability of ZnO is a drawback. Rapid recombination can come from the rapid agglomeration in the bulk form so the ZnO can lose the

Nomenclatures

d	Particle size

Greek Symbols

β	Full width at half-maximum (FWHM)
λ	Wavelength
λ_{edge}	Edge wavelength
θ	Reflection angle

Abbreviations

DRS-UV	Diffuse reflectance Ultra Violet Spectroscopy
JCPDS	Joint Committee of Powder Diffraction Spectra
SEM	Scanning electrone microscope
TEM	Transmission electrone microscope
XRD	X-ray diffraction

activity [1]. As a strategy to overcome the problem is to prepare the ZnO in the nanoscale ZnO or called as ZnO nanoparticle. ZnO nanoparticle research is growing as fast as nanotechnology development. With its small dimension, ZnO nanomaterials are developed for utilization in the next-generation biological applications including cosmetic and sunscreen industry, antimicrobial agents, drug delivery and even in bio-imaging.

Many strategies were reported for creating hierarchical and specific structure and morphology of ZnO since its photocatalytic and biocide properties are reported to be closely related with their physical form. One interesting scheme related to green chemistry approach for the synthesis is the use of plants extracts for the synthesis. The scheme is valued as cost effective and environment friendly easily scaled up for large scale synthesis since it does not need high pressure, temperature and energy and the specific properties one is the use of the renewable agent. Some investigations related to the use of plant and agricultural wastes for the preparation of ZnO nanoparticles are listed in Table 1 [1-10].

By considering some advantageous of agricultural wastes utilization, in this present study, research on the utilization of rice bran powder waste is investigated. Previous investigations reported the utilization of agricultural waste such as sorgum bran, wheat bran, corn cob extract [11-15]. The basic mechanism for the templating ZnO synthesis is related to the content of fibrous biopolymer such as xylan that of obtained from other agricultural wastes [3]. In fact, the potency of rice bran in Asian countries is very high and chemical content of the bran is similar to those that has been reported, this study adopted the utilization of agricultural waste for ZnO NPs synthesis.

The utilization of rice bran extract in synthesis of gold nanoparticles revealed that chemical content in rice brain mainly ferulic acid acted as reducing and stabilizing agent during gold nanoparticles synthesis and the results have significance in as an economic eco-friendly route [14]. Another significant variable parameter in the synthesis of ZnO NPs is the temperature of the formation in that particle size is mainly affected by the temperature in the synthesis.

For photocatalytic application, the particle size gives influence on the band gap energy of particles which is the main character of ZnO NPs photocatalyst. Refer to the mechanism and the effect of temperature as important preparation variable, this study is focusing on the thermal change during ZnO formation using rice bran extract and its effect on the physicochemical character of the ZnO NPs. The photocatalytic was tested for bromophenol blue (BPB) photodegradation while antibacterial activity was performed against *Escherichia coli*, *Staphylococcus aureus* and *Pseudomonas aeruginosa* bacteria.

Table 1. Some researches on ZnO NPs synthesis using plant/agricultural extract.

Plant Extract/Agricultural waste Used	Results	References
Rosa canina	Fast synthesis of ZnO NPs by microwave irradiation	[1]
Aspalathus linearis's extract	high purity crystalline ZnO quasi-spherical nanoparticles by green process using the natural extract of *A. linearis*	[2]
Wheat bran	Low cost synthesis of ZnO NPs with the particle size of about 100 nm	[3]
Pongamia pinnata	The succeed of ZnO NPs with antibacterial activity against *Staphylococcus aureus* and *Escherichia coli*	[4]
Trifolium pratense flower	The succeed of ZnO NPs with antibacterial activity against *Staphylococcus aureus*, *Escherichia coli*, and *P. aeruginosa* and	[5]
Jacaranda mimosifolia flower	the biosynthesis of ZnO NPswith a narrow size range of 2-4 nm using the extract	[6]
Hibiscus rosa-sinensis	Synthesized nano crystallites of ZnO are in the range of 30-35 nm	[7]
Agathosma betulina	The prepared ZnO NPs with quasi-spherical form with 15.8 nm in size	[8]
Tamarindus indica (L.) leaf	ZnO NPs with roughly spherical particles with the size range of 19-37 nm in diameter	[9]
Solanum nigrum leaf extract	The ZnO NPs as a quasi-spherical in shape and their diameter at around 29.79 nm	[10]

2. Materials and Methods

2.1. Materials

Rice bran was obtained from the agricultural area of Sleman District, Special Region of Yogyakarta Province, Indonesia. Sodium hydroxide, ethanol, zinc acetate dehydrate, brom phenol blue (BPB) were obtained from Merck. Rice bran

extract was obtained by immersing the 10g rice bran powder in 100mL of NaOH 10% for 24h and then the supernatant was added with 50mL of ethanol.

2.2. Methods

About 0.1M zinc acetate dihydrate were mixed with 25 ml of extract and followed by refluxing for two hours for complexation reaction. After the reaction completed, the precipitate was dried in an oven at 80^{o}C. The powder obtained by this process was analyzed by DTA-TGA in order to determine the temperature of calcination. ZnO NPs was obtained after calcination at mean temperature.

Thermal transformation of the powder was characterized by XRD, BET surface area, SEM and TEM measurement. XRD Shimadzu X6000 was utilized for measurement with Ni-filtered Cu-Kα as radiation source with the step size of 0.4^{o}/min at the range of 2θ=5-80^{o}. For surface profile analysis consists of specific surface area, pore volume, pore radius and pore distribution, NOVA 1200e was employed. The sample was degassed at 90^{o}C for 2 h prior N_2 adsorption experiment. The surface morphology of prepared material was characterized using FE-SEM (JEOL JSM 6701-F) and TEM Philips. For SEM analysis, the sample was coated on carbon coated copper grid. TEM was operated at an accelerating voltage of 200kV. The sample was coated prior analysis.

2.3. Activity Test

Photocatalytic test of the material was conducted in BPB photodegradation over photocatalysis and photooxidation mechanism. For photooxidation treatment 0.2g of ZnO NPs was added into 500mL of BPB solution in the photocatalytic reactor with the addition of H_2O_2 by the BPB: H_2O_2 mole ratio of 10:1. UV light was exposed to the stirred mixture and the sampling of BPB solution was collected after the treatment for 5; 10; 15; 30; 60; 120 and 180mins. BPB concentration for each sample was determined by using the colorimetric method with UV-Visible spectrophotometry. The photocatalysis treatment is the similar treatment with photooxidation but without the addition of H_2O_2.

Synthesized ZnO was tested for inhibition against *E.coli* and *S.aureus* bacteria. Antibacterial assay were carried out by disc diffusion method. All the bacterial strains were enriched in nutrient broth at 37^{o}C for 18-24 h. Furthermore, they were streaked over the surface of peptone agar by using sterile cotton swabs. 200μg/mL of the ZnO suspension in water was pipetted on a 6 mm sterile paper disc and the solvent was dried before was placed on the surface of the plate for incubation for 24 h at 37 ^{o}C. Antimicrobial activity was measured as the diameter of zone of inhibition excluding the paper disc diameter which was observed after 24 h. Each analysis was performed triplo.

3. Results and Discussion

The thermal conversion of Zn-rice bran complex from the reflux procedure is presented in Fig. 1. The thermogram revealed the weight loss at about 16% at about 200-350 ^{o}C attributed to conversion of moisture and water. The conversion of hydroxyl occurs at the range of 250-300 ^{o}C. Fast degradation occurs at the temperature of 350-430^{o}C indicating the transformation of the organic functional group which may be attributed to the dissociation of precursor react with O_2 to

form CO_2 and H_2O. This is confirmed by the weight loss observed in the temperature region 400-600 °C in the TGA curve.and at the same time the formation of ZnO NPs. At the same temperature DTA curve exhibits the maximum peak indicating the exothermic reaction may relate to dissociation reaction of the organic compound and also transformation of Zn from its hydroxyl form in the organometalic complex to ZnO NPs [5, 16, 17]. From the pattern, it is confirmed that ZnO formation occurs at the thermal transformation at around 430°C. This temperature is pointed out as calcination temperature.

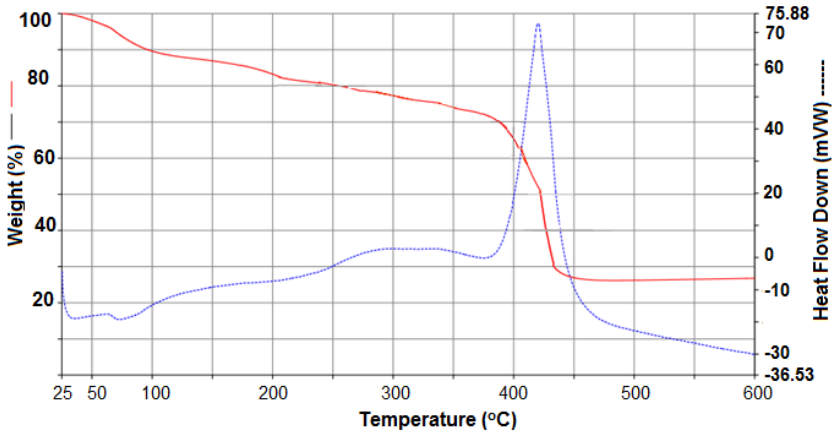

Fig. 1. DTA-TGA thermogram of Zn-rice bran complex.

X-ray diffraction was taken to further confirm the zinc oxide phase of the nanoparticles. The XRD pattern of zinc oxide nanoparticles is shown in Fig. 2. The XRD peaks were identified at (100), (002), (101), (012), (110), (013), (220), (112), and (201) as the indication of ZnO wurtzite (JCPDS card no. 36-1451). The high intense diffraction peaks indicate the well crystalline nature of zinc oxide. Some other peaks are identified as wulfingite $Zn(OH)_2$ (JCPDS card no. 38-0385) indicates that there is an incomplete transformation of ZnO during the synthesis.

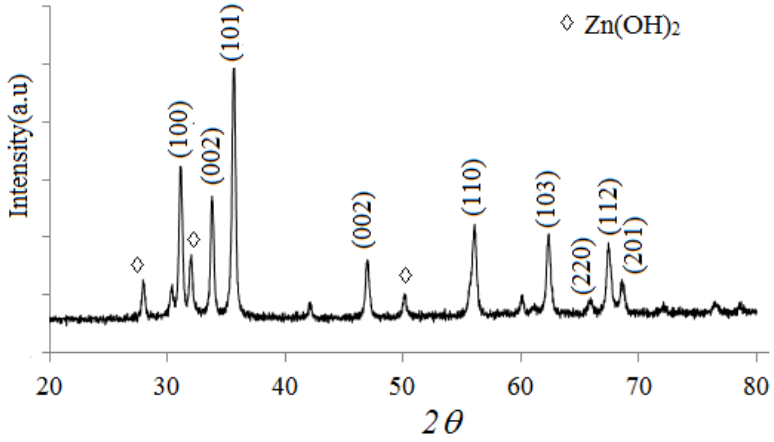

Fig. 2. XRD pattern synthesized ZnO NPs.

The synthesized ZnO nanoparticle diameter was calculated using Debye-Scherrer formula :

$$d = \frac{0.89\lambda}{\beta cos\theta} \quad (1)$$

With 0.89 is Scherrer's constant, λ is the wavelength of X-rays, θ is the Bragg diffraction angle, and β is the full width at half-maximum (FWHM) of the diffraction peak corresponding to plane 101 located at 36.03°. The average particle size of the sample was found to be 17.60 nm which is derived from the FWHM of the more intense peak corresponding to (101) plane located at 35.64◦ using Scherrer's formula.

Figure 3 represents the SEM profile of prepared ZnO NPs at different magnifications. These pictures confirm the formation of ZnO nanoparticles in two forms: amorphous aggregates and needle like form in other parts. A different form may be correlated with different effect of thermal decomposition during calcination. Refer to previous publications, different heating energy creates different form [18, 19]. Since the calcination temperature used in this preparation is 430°C which transitional temperature for $Zn(OH)_2$ to ZnO. From previous investigation, it is found that it is possible to get the growth of ZnO needle-like particles from rhombic $Zn(OH)_2$ from the thermal decomposition. The data are in line with the presence of $Zn(OH)_2$ XRD pattern in Fig. 2.

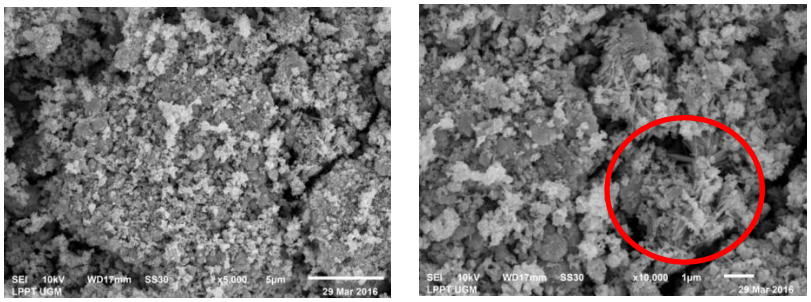

Fig. 3. SEM Profile of ZnO NPs at magnifications of 5000X and 10,000X.

Surface parameter of the ZnO NPs consists of specific surface area, BJH pore volume and BJH pore radius parameters are determined by adsorption-desorption profile in Fig. 4. From calculation, the specific surface area, BJH pore volume and BJH pore radius are 33.61 m^2/g, 0.89 cc/g and 22.34 nm respectively.

The nitrogen adsorption-desorption isotherms for ZnO NPs in Fig. 4 as type IV according to IUPAC classification, indicating mesopores structure of the material. Moreover, its H3 type hysteresis loop representing aggregates as also confirmed by TEM profile (Fig. 5). The average pore radius of the sample is 22.34 nm. The result is in the similar range pore radius as reported by the investigation on ZnO NPs preparation using rice as soft biotemplate [20]. From the picture, it is confirmed that the nanoparticles are not uniform as also reported by the utilization of plant extract as bioreductor in affecting heterogeneous form [21]. The similar mechanism may apply for the complex formation and thermal conversion during calcination.

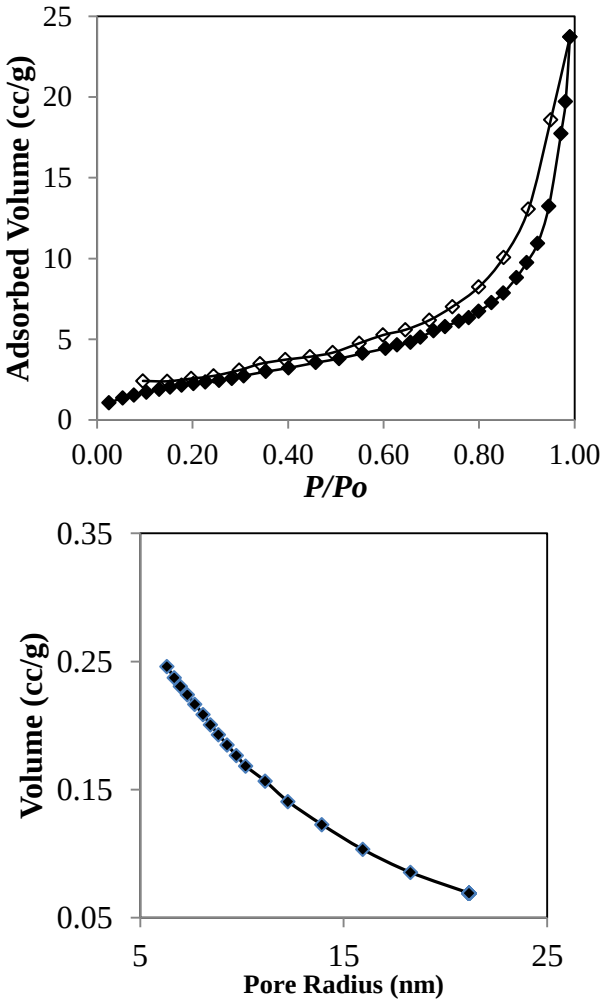

Fig. 4. (a) Adsorption-desorption and (b) Pore radius distribution profile of prepared ZnO NPs.

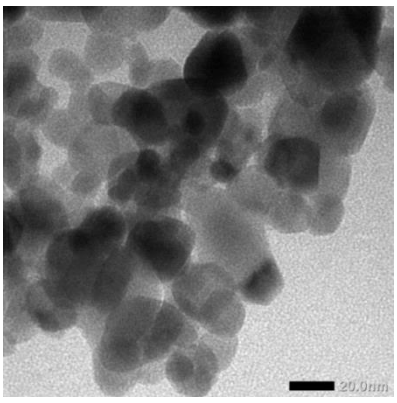

Fig. 5. TEM profile of material.

Moreover the UV-DRS spectra of the material presented in Fig. 6 indicating the λ_{edge} of 389.9 nm correspond to the value of 3.18 eV. The value suggests that the material has the band gap potential for photocatalytic application refer to its capability to absorb photon in the mechanism.

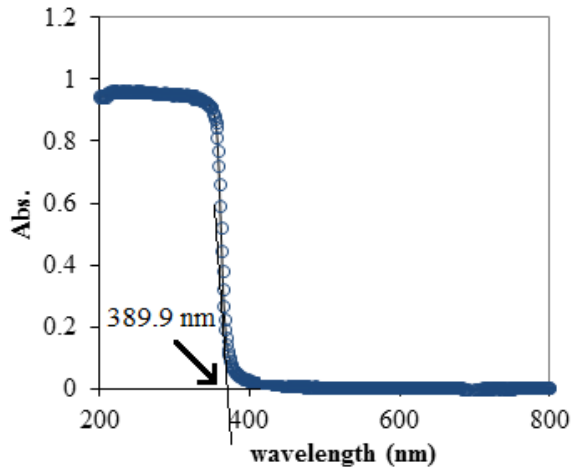

Fig. 6. UV-DRS spectra of the material.

Photocatalytic activity of prepared ZnO NPs was performed in varied treatments of BPB: photooxidation, photocatalysis and adsorption. The difference between photocatalysis and photooxidation treatment is on the addition of H_2O_2 as oxidant in the system for accelerating the oxidation. The mechanism of photocatalysis over ZnO is as follow:

$$ZnO+h\nu \rightarrow ZnO(e^-_{(CB)}+h^+_{(VB)})$$

$$O_{2ads}+e^- \rightarrow O^{\bullet -}_{2ads}$$

$$O^{\bullet -}_{2ads}+H^+ \rightarrow HO_{2ads}$$

$$O^{\bullet -}_{2ads}+2H^++e^- \rightarrow H_2O_{2ads}$$

$$R_{ads}+h^+ \rightarrow R^{\bullet}_{ads}{}^+$$

$$HO^-_{ads}+h^+ \rightarrow \bullet OH_{ads}{}^+$$

$$H_2O_{ads}+h^+ \rightarrow .OH_{ads}+H^+$$

As the photon expose to the ZnO, there is an excitation of electrone from valence band to conductance band and leave hole (h^+) due to the capability of ZnO to chatch photon due to its band gap energy. Interaction between oxygen and exiting electrone produces oxygen radicals and in same time, hydroxy radicals will be produced from the interaction of hole (h+) and hydroxyl from solvent. The radicals play important role for oxidizing organic compound. The presence of hydrogen peroxide accelerate the oxidation via faster oxygen radicals formation.

From the kinetic of BPB degradation (Fig. 7) it is confirmed that the material shows the photocatalytic activity in that the rate of BPB degradation by using photooxidation is higher compared to photocatalysis. Moreover, both treatments

give higher rate compared to adsorption in that there is no UV light neither H_2O_2 oxidant so the BPB reduction is only related with the surface area of ZnO NPs. The presence of BPB reduction by oxidation reaction is also expressed by the UV-Visible spectra. Along as the increasing time of photocatalytic treatment, the changes of not only concentration but also the components in the treated solution is appeared by the loss of peak at around 597 nm followed by the reduction of intensity and also shift of the peak at 310 nm. In general the ZnO NPs exhibits photocatalytic activity which is closely related to the band gap energy value (3.18 eV) as the responsible parameter in photocatalysis mechanism.

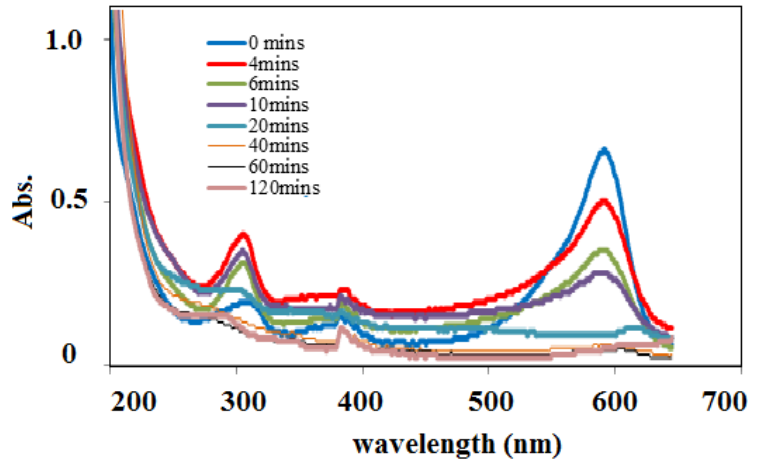

(a)

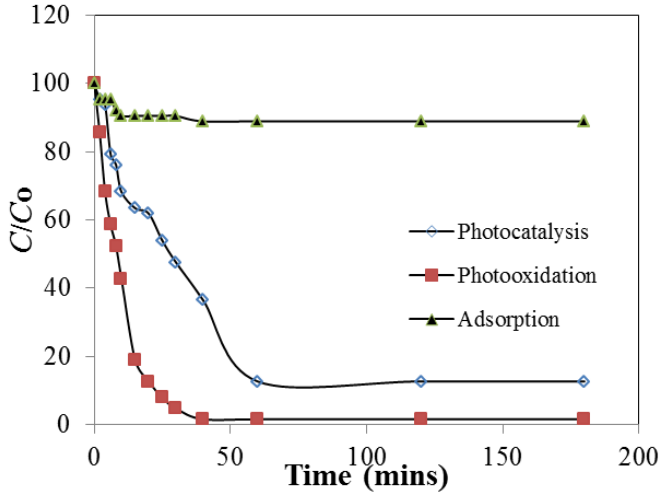

(b)

Fig. 7. (a) UV-Visible spectra of initial and treated solution of BPB (b) Kinetics of BPB degradation over varied treatments [initial concentration of BPB=10ppm].

From the antibacterial activity it is found that the ZnO NPs demonstrates antibacterial activity for all tested microbes although the inhibition zones are lower than the positive control (chloramphenicol) (Table 2). It is also found that the material exhibits the activity against *P.aeruginosa* rather than two other bacteria. Although many publications proofed the antibacterial activity of, ZnO NPs, the fix antibacterial mechanism is not clear. Many hypothesis predict that the actvivity is established from the release of Zn^{2+} ions and enhance reactive oxygen speciess (ROS) production that furthermore attack the bacteria. The antibacterial activity data of prepared material againts *S.aureus* is also lower compared to synthesized ZnO NPs previously reported by using Pomangia *Pongamia pinnata* and *Trifolium pratense* flower extract [4, 5]. The significant difference of inhibition zone was influenced by many factors such as morphology, particle size and condition of analysis.

Table 2. Inhibition zone data of ZnO NPs antibacterial activity against tested bacteria.

Antibacterial agent	Inhibition zone (mm)		
	S.aureus	***E.coli***	***P.aeruginosa***
ZnO NPs	7.3±0.05	7.6±0.1	8.25±0.1
Cloramphenicol (Control +)	23.6±0.1	23.8±0.2	10.4±0.05

4. Conclusion

From the physicochemical character studies and the activity test it can be concluded that the preparation of ZnO NPs using rice bran as renewable and low cost templating agent has been successfully conducted. The data from the XRD and TEM measurement represents the particle size of ZnO NPs at particle size of 17.60 nm and exhibits the photocatalytic activity as related to the band gap energy value of 3.18 eV. The material also shows the antibacterial activity against *Eschericia coli*, *Staphylococcus aureus* and *Pseudomonas aeruginosa* bacteria.

References

1. Jafarirad, S.; Mehrabi, M.; Divband, B.; and Kosari-Nasab, M. (2016). Biofabrication of zinc oxide nanoparticles using fruit extract of Rosa canina and their toxic potential against bacteria: A mechanistic approach. *Materials Science and Engineering: C*, 59, 296-302.
2. Diallo, A.; Ngom, B.D.; Park, E.; and Maaza, M. (2015). Green synthesis of ZnO nanoparticles by Aspalathus linearis: Structural & optical properties. *Journal of Alloys and Compounds*, 646, 425-430.
3. Harish, B.S.; Uppuluri, K.B.; and Anbazhagan, V. (2015). Synthesis of fibrinolytic active silver nanoparticle using wheat bran xylan as a reducing and stabilizing agent. *Carbohydrate Polymers*, 132, 104-110.

4. Sundrarajan, M.; Ambika, S.; and Bharathi, K. (2015).Plant-extract mediated synthesis of ZnO nanoparticles using Pongamia pinnata and their activity against pathogenic bacteria. *Advanced Powder Technology,* 26(5), 1249-1299.
5. Dobrucka, R.; and Długaszewska, J. (2015). Biosynthesis and antibacterial activity of ZnO nanoparticles using Trifolium pratense flower extract. *Saudian Journal of Biological Sciences,* 23(4),517-523.
6. Sharma, D.; Sabela, M.I.;Kanchi, I.Mdluli, P.S.; Singh, G., Stenström, T.A.;Bisetty, K. (2016). Biosynthesis of ZnO nanoparticles using Jacaranda mimosifolia flowers extract: Synergistic antibacterial activity and molecular simulated facet specific adsorption studies. *Journal of Photochemistry and Photobiology B: Bioogy,* 162, 199-207.
7. Devi, R.; and Gayathri, R. (2014). Green Synthesis of Zinc Oxide Nanoparticles by using Hibiscus rosa-sinensis. *International Journal of Current Engineering and Technology,* 44, 2444-2446.
8. Thema, F. T.; Manikandan, E.; Dhlamini, M. S.; andMaaza, M. (2015). Green synthesis of ZnO nanoparticles via Agathosma betulina natural extract. *Material Letters,* 161, 124-127 (2015).
9. Elumalai, K.; Velmurugan, S.; Ravi, S.; Kathiravan, V.; and Ashokkumar, S. (2015). Facile, eco-friendly and template free photosynthesis of cauliflower like ZnO nanoparticles using leaf extract of Tamarindus indica (L.) and its biological evolution of antibacterial and antifungal activities. *Spectrochimica Acta - Part A Molecular and Biomolecular Spectroscopy,* 136, 1052-1057.
10. Ramesh, M.; Anbuvannan, M.; and Viruthagiri, G. (2015). Green synthesis of ZnO nanoparticles using Solanum nigrum leaf extract and their antibacterial activity. *Spectrochimical Acta - Part A Molecular and Biomolecular Spectroscopy,* 136, 864-870.
11. Sharma, D.; Kanchi, S.; andBisetty, K. (2015). Biogenic synthesis of nanoparticles: A review. *Arabian Journal of Chemistry,* article in press. doi:10.1016/j.arabjc.2015.11.002
12. Gupta, S.; Jangir, O. P.; andSharma, M. (2016). The Green Synthesis, Characterization and Evaluation of Antioxidant and Antimicrobial Efficacy of Silver and Gold Nanospheres Synthesized Using Wheat Bran, *Asian Journal of Pharmacetical and Clinical Research,* 9, 103-106.
13. Okoronkwo, E. A.; Imoisili, P. E.; Olubayode, S. A.; and Olusunle, S. O. O. (2016). Development of Silica Nanoparticle from Corn Cob Ash. *Advance in Nanoparticles,* 5, 135-139.
14. Malhotra, A.; Sharma, N.; Navdezda; Kumar, K.; Dolma, K.; Sharma, D.; Nandanwar, H.S.; and Choudhury, A.R. (2014). Multi-analytical approach to understand biomineralization of gold using rice bran: A novel and economical route. *RSC Advance,* 4, 39484-39490.
15. Shah, M.; Fawcett, D.; Sharma, S.; Tripathy, S. K.; and Poinern, G. E. J. (2015). Green synthesis of metallic nanoparticles via biological entities. *Materials,* 8, 7278-7308. .
16. Khalil, M. I.; Al-Qunaibit, M. M.; Al-zahem, A. M.; andLabis, J. P. (2014). Synthesis and characterization of ZnO nanoparticles by thermal decomposition of a curcumin zinc complex. *Arabian Journal of Chemistry,* 7, 1178-1184.

17. Moezzi, A.; Cortie, M.; Mcdonagh, A. (2016). Transformation of zinc hydroxide chloride monohydrate to crystalline zinc oxide. *Dalton Transactions*, 5, 7385-7390.
18. Hasanpoor, M.; Aliofkhazraei, M.; Delavari, H. (2015). Microwave-assisted Synthesis of Zinc Oxide Nanoparticles. *Procedia Material Sciences*, 11, 320-325.
19. Wang, M.; Zhou, Y.; Zhang, Y.; Hahn, S. H.; andKim, E. J. (2011). From $Zn(OH)_2$ to ZnO: a study on the mechanism of phase transformation. *CrystEngComm.*, 13, 6024-6026..
20. Ramimoghadam, D.; Bin Hussein, M. Z.; and Taufiq-Yap, Y. H. (2013). Hydrothermal synthesis of zinc oxide nanoparticles using rice as soft biotemplate. *Chemistry Central Journal*, 7, 136-139. (2013).
21. Narendhran, S.; Rajivi, P.; Sivaraj, R. (2016). Influence of Zinc Oxide Nanoparticles on Growth of *Sesamum indicum L.* in Zinc Deficient Soil. *International Journal of Pharmacy and Pharmaceutical Sciences*, 8, 365-371.